



Sulfated Small Molecules Targeting EBV in Burkitt Lymphoma: From *In Silico* Screening to the Evidence of *In Vitro* Effect on Viral Episomal DNA

Raquel T. Lima^{1,2,†}, Hugo Seca^{1,3,†},
 Andreia Palmeira^{1,2,4}, Miguel X. Fernandes⁵,
 Felipe Castro^{2,4}, Marta Correia-da-Silva^{2,4},
 Maria S. J. Nascimento^{2,3}, Emília Sousa^{2,4},
 Madalena Pinto^{2,4} and M. Helena Vasconcelos^{1,3,*}

¹Cancer Drug Resistance Group, IPATIMUP – Institute of Molecular Pathology and Immunology of the University of Porto, Porto, Portugal

²CEQUIMED-UP, Centre of Medicinal Chemistry – University of Porto, Porto, Portugal

³Department of Biological Sciences, Laboratory of Microbiology, Faculty of Pharmacy, University of Porto, Porto, Portugal

⁴Departamento de Ciências Químicas, Laboratório de Química Orgânica e Farmacêutica, Faculdade de Farmácia, Universidade do Porto, Porto, Portugal

⁵Centro de Química da Madeira, Centro de Competência de Ciências Exactas e da Engenharia, University of Madeira, Funchal, Portugal

*Corresponding authors: M. Helena Vasconcelos, hvasconcelos@ipatimup.pt; E. Sousa, esousa@ff.up.pt

†These authors equally contributed to this work.

Epstein–Barr virus (EBV) infects more than 90% of the world population. Following primary infection, Epstein–Barr virus persists in an asymptomatic latent state. Occasionally, it may switch to lytic infection. Latent EBV infection has been associated with several diseases, such as Burkitt lymphoma (BL). To date, there are no available drugs to target latent EBV, and the existing broad-spectrum antiviral drugs are mainly active against lytic viral infection. Thus, using computational molecular docking, a virtual screen of a library of small molecules, including xanthenes and flavonoids (described with potential for antiviral activity against EBV), was carried out targeting EBV proteins. The more interesting molecules were selected for further computational analysis, and subsequently, the compounds were tested in the Raji (BL) cell line, to evaluate their activity against latent EBV. This work identified three novel sulfated small molecules capable of decreasing EBV levels in a BL. Therefore, the *in silico* screening presents a good approach for the development of new anti-EBV agents.

Key words: antivirals, Burkitt lymphoma, Epstein–Barr virus, sulfated small molecules, virtual screening

Received 24 May 2012, revised 13 November 2012 and accepted for publication 8 January 2013

Epstein–Barr virus (EBV) infection has been associated with several human malignancies, including Burkitt lymphoma (BL), as EBV is responsible for transforming B cells and contributing to their malignant phenotype. Epstein–Barr virus is a 184-kbp double-stranded DNA linear genome virus which, once in the nucleus of infected cells, circularizes adopting an episomal shape (1). Epstein–Barr virus episome presents two origins of replication, *oriP* and *oriLyt*, which are used to replicate the virus genome during its latent or lytic phase, respectively. Epstein–Barr virus may adopt different types of latency (mainly type I, II, and III) during the latent phase of infection, depending on the proteins expressed (2). In type I latency, a very restricted number of latent proteins are expressed, whereas in type III latency, all set of latent proteins are expressed. Epstein–Barr virus nuclear antigen 1 (EBNA1) is the only latent protein that is expressed in all types of latencies. Importantly, the association of this protein with the *oriP* sequence is required for both initiation and maintenance of replication of EBV episomes in infected cells (3–5). Moreover, EBNA1 is also able to regulate its own expression (6) and, by binding to *oriP*, to enhance transcription from several viral promoters, such as the LMP1 promoter, leading to the regulated expression of other latent proteins (7). The replication of EBV episomal DNA also requires cellular proteins, such as DNA polymerase, which is not sensitive to antiviral drugs (8).

The switch from latency to lytic phase may occur following different stimulus (9–13). The expression of the immediate-early protein Zta was found to trigger viral lytic replication by activating several promoters, therefore leading to the expression of early lytic genes such as the early-antigen-diffuse component (EA-D), the EBV DNA polymerase (involved in viral DNA replication), and the BamHI fragment H rightward open reading frame 1 (BHRF1, an anti-apoptotic molecule homologue of cellular Bcl-2). Following this stage, the expression of late EBV proteins involved in the structure of the virus will occur, and viral DNA replication will not depend on the cellular machinery anymore. Completion of the viral lytic cycle results in the production of

new infectious viruses that will ultimately lead to cell death and viral dissemination.

As latent EBV is associated with the development of various diseases and because in therapeutics there are no available drugs to target latent EBV, the development of such compounds is necessary. In fact, even though there are some broad-spectrum antiherpes drugs available, which might be used against EBV, they are only active in the lytic phase of EBV infection (8). This is due not only to the fact that EBV episomal replication depends on the host cellular machinery to occur, but also to the fact that some antiviral drugs such as ganciclovir need to be processed by lytic viral proteins to become active (14,15). Therefore, as most EBV+ tumor cells (such as BL cells) have latent EBV, they are resistant to these known antiviral drugs (8). Thus, there is a strong need for the development of new antiviral agents that can target cells that have the virus in a latent state and that do not depend on the reactivation of the virus.

Some strategies have been proposed to target latent EBV. For example, hydroxyurea (HU) leads to EBV episome loss from cells and has been efficiently used *in vitro* (16) as well as *in vivo*, in the treatment of EBV-associated primary central nervous system lymphoma (17). However, this drug has the disadvantage of leading to the accumulation of additional mutations in the cellular genome (18). Other approaches, using antisense, RNAi, or DNAszymes strategies to downregulate viral oncoproteins such as LMP1 *in vitro*, have been shown to decrease proliferation and to increase sensitivity to apoptotic stimulus in the treated cells (19,20). In addition, viral lytic replication was shown to be reduced following downregulation of LMP2B by RNAi (21).

Several natural and synthetic compounds, including flavonoids (22–25), xanthenes (26), and other small molecules (27–30), have been described to have antiviral activity against EBV. The purpose of the current study was to identify compounds with antiviral activity against EBV, by carrying out an *in silico* screen of molecules from a library of flavonoids and xanthenes from the CEQUIMED-UP research center using computational molecular docking and to further investigate their effect *in vitro* in an EBV+ BL cell line. Our results depict the advantages of strategies combining computational analysis with biological studies in the search for new antiviral agents and show evidence of antiviral activity against EBV for the three sulfated compounds studied.

Methods and Materials

Docking of in-house molecules

Structures of several EBV proteins were collected from Protein Data Bank (PDB) (31), namely EBNA1 (PDB IDs *1b3t* and *1vhi*), Zta (PDB IDs *2c9l* and *2c9n*), and BHRF1

(PDB ID *1q59*). Virtual screening was carried out on a commodity PC running Linux Ubuntu 6.06. The software eHITS 2009 from SimBioSys Inc (32,33) was used for active site detection and docking. Hyperchem from HyperCube Inc (34) was used to draw and optimize 97 structures from CEQUIMED-UP library. No special preparation of the 3D structures was carried out because eHITS automatically evaluates all of the possible protonation states for ligands and receptor. eHITS was run using the DNA-binding residues as clip files, and the docking is performed, by default, within a 7-Å margin around them. The docking accuracy was set to 2, the number of docking poses was set to 5, and SDF was chosen as the output file format. A multiple active site correction (MASC) was applied to the obtained docking scores (35). Open Babel (36) was used to manipulate the various file formats of ligands. PyMol from DeLano (37) and chimera from UCSF (38) were used for visual inspection of results and graphical representations. Pymol 'list_contacts' script (cut-off = 4.0 Å) was used to determine possible contacts between the receptor and the ligand. For docking validation, a set of 150 molecules obtained from NCI database (39) were also docked to the several EBV proteins in the same conditions as previously described for the in-house molecules.

Tested compounds

The synthesis of 3,6-di(3',4',5',6'-*O*-tetrasulfate- β -*D*-glucopyranosyl)-xanthone (**1**), diosmin 2'',2''',3'',3''',4'',4'''-*O*-hexasulfate (**2**), and mangiferinpersulfate (**3**) resulted from the sulfation of diglycosylated 3,6-dihydroxyxanthone (40), diosmin (D3525; Sigma-Aldrich, Sintra, Portugal), and mangiferin (M3547; Sigma-Aldrich), respectively, as previously described (41,42). The purity (>95%) of each compound (**1–3**) was determined by HPLC-DAD analysis. Compounds **1–3** were dissolved in H₂O. 12-*O*-Tetradecanoylphorbol-13-acetate (TPA), a known EBV lytic-inducing agent, was purchased from Calbiochem (Darmstadt, Germany) and dissolved in DMSO.

Cell culture

The BL cell line, Raji, was used. Cells were cultured in RPMI 1640 with Glutamax supplemented with 10% fetal bovine serum (Gibco, Invitrogen, Paisley, UK) and incubated in a humidified incubator at 37 °C with 5% CO₂ in air.

Cell treatment with the tested compounds

Raji cells (5×10^5 /mL) were treated with 20 μ M of compounds **1–3** for 48 h or 96 h. In the studies to analyze viral reactivation, 5×10^5 Raji cells/mL were incubated with 30 ng/mL TPA alone or simultaneously with 20 μ M of each compound (**1–3**). The effect of the DMSO or H₂O vehicle solvents (controls) or of medium (blank) was evaluated in all experiments. Viable cell number was counted using the trypan blue exclusion assay.

DNA extraction and EBV DNA analysis

DNA was extracted from Raji cells following 96-h incubation with the tested compounds (**1–3**), as previously described in (43). Analysis of the EBV DNA load was carried out with conventional PCR and with real-time quantitative PCR using the following primers: (i) EBV DNA 5' CGGTGCGCCAGTCCTACCAG 3' and 5' CCTGGAGAGGTCAGGTTACT-3' (44) and (ii) actin 5'-GCCATGGTTGTGCCATTACA-3' and 5'-GGCCAGGTTCTCTTTTATTTCTG-3' (45). For the conventional PCR, conditions were the following: 95 °C for 5 min, 35 cycles of amplification (95 °C for 30 seconds, 56 °C for 30 seconds, and 72 °C for 30 seconds), and a final extension step of 72 °C for 10 min. PCR products were then electrophoresed on 2% agarose gels containing GelStar (Lonza, Rockland, ME, USA). Densitometry analysis was carried out by quantifying the intensity of the bands using the software Quantity One – 1D Analysis (Bio-Rad, Hercules, CA, USA). For real-time PCR, the Fast SYBR[®] Green Master Mix (Applied Biosystems, Paisley, UK) was used according to manufacturer's instructions. A standard curve was prepared using serial dilutions of Raji cells' DNA. A dissociation curve was generated for each set of primers, and a single peak was obtained; additionally, the PCR efficiency was estimated as being always higher than 95%. EBV DNA levels were normalized for cellular DNA (actin), to exclude any possible cytotoxic effect of the molecules.

Protein isolation, quantification, and Western blot

Total protein lysates were prepared from cells following 48-h incubation with compounds **1–3** as described in (13, 46). Protein (20 µg) was subjected to SDS–PAGE (in 12% Bis-tris gel), transferred onto a nitrocellulose membrane (GE Healthcare, Buckinghamshire, UK), and incubated with the following primary antibodies: mouse EA-D antibody (1:1000; Millipore, Billerica, MA, USA), mouse LMP-1 antibody (1:100, CS1-4 clone; DAKO, Glostrup, Denmark), or goat actin antibody (1:2000; Santa Cruz Biotechnology, Heidelberg, Germany). The membrane was then incubated with one of the following secondary antibodies: goat anti-mouse IgG-HRP (1:2000; Santa Cruz Biotechnology, Heidelberg, Germany) or donkey anti-goat IgG-HRP (1:2000; Santa Cruz Biotechnology). Signal was detected with the ECL Western blot Detection Reagents (GE Healthcare), the Amersham Hyperfilm ECL (GE Healthcare), and the Kodak GBX developer and fixer (Sigma, St. Louis, MO, USA) (46,47).

Results

Three proteins were selected for the docking studies (latent EBNA1, immediate-early Zta, and lytic BHRF1). The reason for choosing these targets was as follows: (i) targeting EBNA1 has been suggested to be a potential strategy to affect latent EBV as this protein is essential in both initiation and maintenance of EBV episome replication and is also the only EBV latent protein present in nearly all

EBV-infected cells; (ii) the expression of the immediate-early lytic protein Zta is sufficient for viral lytic reactivation, and therefore, its targeting may result in lytic cycle inhibition with no viral particles being produced; accordingly, the use of antisense and RNAi technologies to reduce Zta expression has been proven to effectively inhibit the EBV lytic cycle *in vitro* (48–50), and (iii) the early lytic protein BHRF1 is transiently expressed in early infection and has anti-apoptotic functions (it is an homologue of cellular Bcl-2) (51); in fact, BHRF1 may protect EBV-infected cells by inhibiting apoptosis to maximize viral production; thus, inhibitors directed to this viral target would probably trigger apoptosis of infected cells.

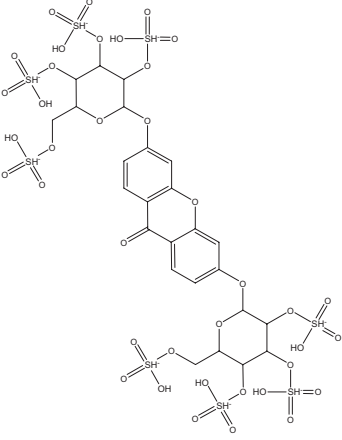
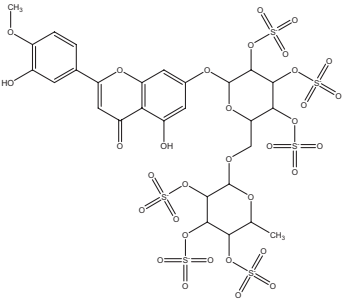
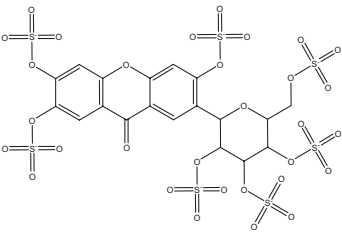
Docking using eHiTS[®]

Docking procedure resulted in a list of potential EBV inhibitors ranked according to the eHiTS scoring function. The total number of compounds screened was 97. These small molecules correspond mainly to xanthenes and flavonoids (90) with diverse substituents such as hydroxy (28), prenyl (15), amine (22), sulfate (16), and others. Only the top three molecules (**1–3**, Table 1) were chosen for further computational analysis. Based on preliminary studies with five of the best molecules in cell lines, in which two of them (non-sulfated derivatives) presented no activity (data not shown), the same top three molecules were then further evaluated *in vitro* with biochemical assays. To comply with disclosure of information agreement, results from 94 of those compounds cannot be presented here.

As docking scores come from several targets, it is not possible to establish a direct comparison (only possible within the same protein and same binding site). Therefore, a MASC score was also given as previously described (35): $MASC = (S_{ij} - \mu_i) / \sigma_i$, where S_{ij} is the original score, μ_i and σ_i are the mean and standard deviation of the scores for compound i . Calculation of mean and standard deviation was made using the docking scores obtained, and results are presented in Table 2. This statistical correction greatly increases the accuracy of ligand scoring and reduces the error of docking studies. Multiple active site correction is different for each molecule, and it is specific for the docking program and scoring function used. Multiple active site correction scores (Table 2) help to understand the most probable target protein for each small molecule tested. Compounds **1–3** all dock to Zta proteins (*2c9n* or *2c9l*), whereas compound **3** is the only compound that docks to EBNA1 receptors (*1b3t*).

Afterward, a careful visual inspection of the SDF files from the best scored ligands on each of the three receptors, EBNA1, Zta, and BHRF1, was performed. As shown in Figure 1A,B, the best fitting molecule (compound **3**) adopted several poses within the DNA-binding groove of EBNA1, filling the space supposedly occupied by the DNA double-strand helix. As far as EBV immediate-early transcription

Table 1: Docking scores (kcal/mol) for the three top molecules (**1–3**) against EBV target proteins: EBNA1 (*1b3t* and *1vhi*), BHRF1(*1q59*), and Zta(*2c9l* and *2c9n*)

Ligand	Docking score on receptor (kcal/mol)				
	EBNA1		BHRF1	Zta	
	<i>1b3t</i>	<i>1vhi</i>	<i>1q59</i>	<i>2c9l</i>	<i>2c9n</i>
 <p>1</p>	–	–	–	–10.641	–11.624
 <p>2</p>	–	–	–	–9.583	–8.825
 <p>3</p>	–8.864	–	–	–8.706	–9.160

EBNA1, Epstein–Barr virus nuclear antigen 1.

factor Zta is concerned, as shown in Figure 1C, D, the best scoring molecules occupy a cavity formed by the two homologous chains X and Y. This binding pocket is the cavity used by the protein to bind to the EBV gene. As for BHRF1, docking was performed in a cavity flanked by residue ASN-61, described as forming the cavity where other proteins from the apoptotic pathway bind (52,53). However,

none of the studied molecules on Table 1 was able to dock to BHRF1, the Bcl-2 homologue from EBV (54).

Docking validation

The NCI database, with more than 250 000 molecules, was used to randomly select 150 compounds. They were

Table 2: Multiple active site correction (MASC) scores

	MASC scores				
	<i>1b3t</i>	<i>1vhi</i>	<i>1q59</i>	<i>2c9l</i>	<i>2c9n</i>
1	–	–	–	0.71	–0.71
2	–	–	–	–0.71	0.71
3	0.20	–	–	0.89	–1.08

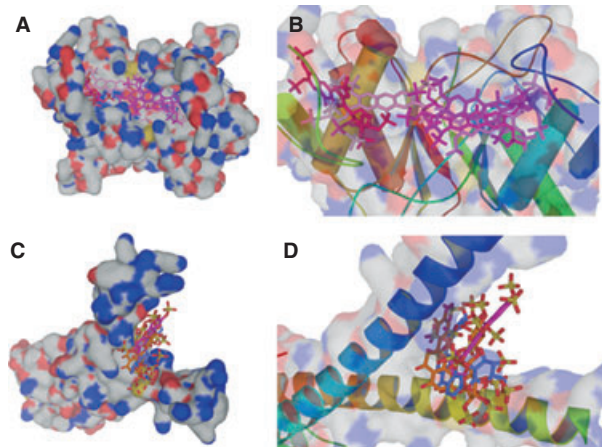


Figure 1: Surface (A) and ribbon and transparent surface (B) representation of Epstein–Barr virus (EBV) nuclear antigen 1 (EBNA1; pdb: *1b3t*) and best ranking poses of compound **3** (several tones of pink). Surface (C) and ribbon and transparent surface (D) representation of Zta protein (pdb: *2c9n*) and best ranking poses of compound **1** (purple), **2** (orange), and **3** (pink). Surfaces are colored by element: gray for carbons, blue for oxygen, and yellow for sulfur.

used as ‘decoy’ ligands to retrospectively validate docking calculations performed for 97 in-house molecules. Each compound from the NCI was docked to proteins with PDB IDs *1b3t*, *1vhi*, *1q59*, *2c9l*, and *2c9n* using eHiTs. As we have several structures for each target protein, this calculation allows us to determine which target structure discriminates better ‘decoy’ from active molecules. Docking validation results using NCI molecules are given in Table S1. Regarding EBNA1 structures (*1b3t* and *1vhi*), *1b3t* was the best one; however, all of the decoy molecules presented a score worse than the score of compound **3** (Table 1). Regarding Zta structures (*2c9l* and *2c9n*), *2c9n* was better in distinguishing ‘decoy’ from active molecules. So, *1b3t* and *2c9n* target structures were used to analyze important residues involved in the binding.

Analysis of best ranked molecules’ docking poses

The docking poses of all active compounds and possible interactions established within the active site of the analyzed EBV targets were carefully inspected.

Epstein–Barr nuclear antigen 1 (EBNA1) binds to four recognition sites in the minimal origin of latent DNA

replication of Epstein–Barr virus and activates latent-phase replication of the viral genomes. Both *1b3t* and *1q59* files are composed of two identical chains, X and Y, and the crystallographed residues 459–607 or 470–607 (in *1b3t* and *1hiv*, respectively) correspond to the DNA-binding and dimerization domains. Epstein–Barr virus nuclear antigen 1 appears to bind DNA via two independent regions termed the core and the flanking DNA-binding domains. The core DNA-binding domain comprises both the dimerization domain and a helix predicted to bind the inner portion of the EBNA1 DNA recognition element. The flanking DNA-binding domain consists in part of an α -helix whose N-terminus contacts the outer regions of the EBNA1 DNA recognition element (55).

Initially, the general shape and polar/apolar main groups from the targets binding site were analyzed, as seen in Figure 2A. Three evident polar evaginations (P1, P2, and P5) and two polar groups (P3 and P4) were present. Two large hydrophobic regions (H1 and H2) also defined the

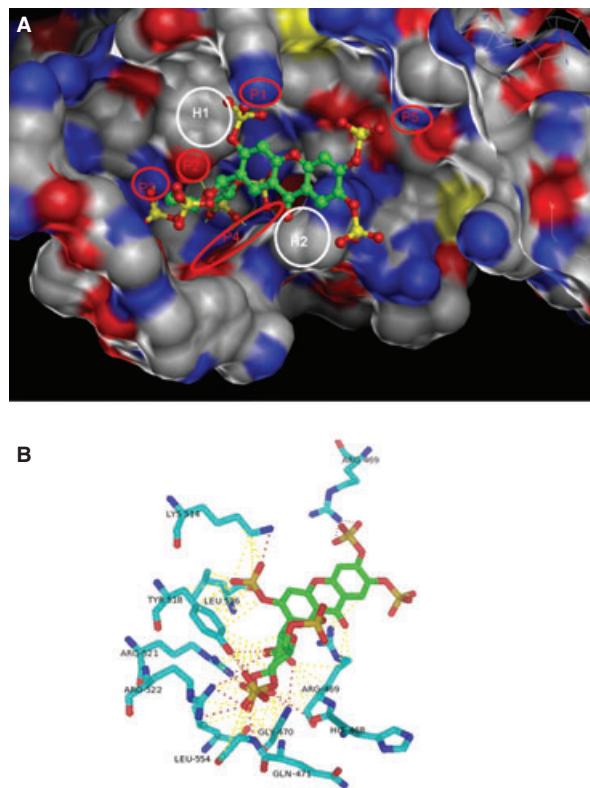


Figure 2: (A) Detail of the Epstein–Barr virus (EBV) nuclear antigen 1 (EBNA1; pdb: *1b3t*) DNA-binding pocket. Compound **3** is docked in the cavity as an example. Regions P1 to P5 represent polar groups important for the establishment of hydrogen interactions; regions H1 and H2 represent hydrophobic regions. Surface is colored by element (red for oxygen, blue for nitrogen, yellow for sulfur, and gray for carbon). (B) Detail of compound **3** bound to EBNA1 (pdb: *1b3t*). Red dashes represent hydrogen interactions, yellow dashes represent other interactions.

walls of the binding pocket. In fact, LYS514 represents polar region P1 and ARG469 represents region P5, whereas LEU536 occupies region P2 and ARG522 occupies region P3. GLY450 and ARG469 form the polar ground P4; on the other hand, the hydrocarbon chains on TYR518, LEU536, and ARG521 form the hydrophobic region H1 and ARG469 form region H2.

For better understanding of the most probable and important residues involved in the binding of EBNA1 inhibitors to EBNA DNA-binding pocket, compound **3** interactions were thoroughly analyzed as seen in Figure 2B. Amine groups present in ARG469, LYS514, ARG521, ARG522, GLN471, and GLY470, as well as a phenol group in TYR518, seem to be responsible for the establishment of H-bond interactions between ligand and target. Other type of interactions may occur, such as dipole-induced dipole interactions between polar groups in the ligand and induced dipoles in LYS514, LEU536, ARG521, LEU554, GLY480, GLN471, and ARG469 carbon chains seem to occur. The presence of a scaffold filling the EBNA1 DNA cavity and the presence of polar groups in strategic positions to establish hydrogen interactions with polar nitrogen and oxygen atoms of the amino acids surrounding that cavity would be an interesting strategy for the design of more potent EBV inhibitors. Involvement of some residues, such as TYR518, LYS514, and ARG469, had already been published as being important in the establishment of polar contacts, which reinforces these findings (56). As highlighted in Figure 2B, compound **3** has sulfate groups that can establish hydrogen interactions or even ion–dipole interactions with the polar amino acids on the walls of EBNA1 DNA-binding pocket.

Regarding the immediate-early transcription factor Zta, its structure was hypothesized to allow the design of new agents that block activation of the EBV lytic cycle by occupying the DNA-binding pocket (57). *2c9n* and *2c9/pdb* files present the crystal structure of Zta's DNA-binding domain (residues 175–236, chains X and Z) bound to an EBV lytic gene promoter element. As seen in Figure 1D, the best fitting small molecules occupy exactly the same place as DNA, thus blocking EBV transcription, and therefore blocking the production of new virions. Analysis of the shape and characteristics of that site (Figure 3A) reveal the presence of two pairs of symmetric evaginations, P1–P2 and P3–P4. A polar sulfur region in P5, as well as polar region P6, is also relevant. A large hydrophobic cavity H1 is also easily detected. Comparing Figure 3A,B, it emerges that ARG190 from chains X and Z are represented in regions P1 and P2, whereas LYS194 from chains X and Z are represented in regions P3 and P4. P5 corresponds to CYS189 and P6 to SER186. The large hydrophobic cavity H1 corresponds to aromatic rings in both PHE193 residues.

Compound **1** was used as an example to analyze the possible interactions (Figure 3B). Guanidine group [–NHC(NH)

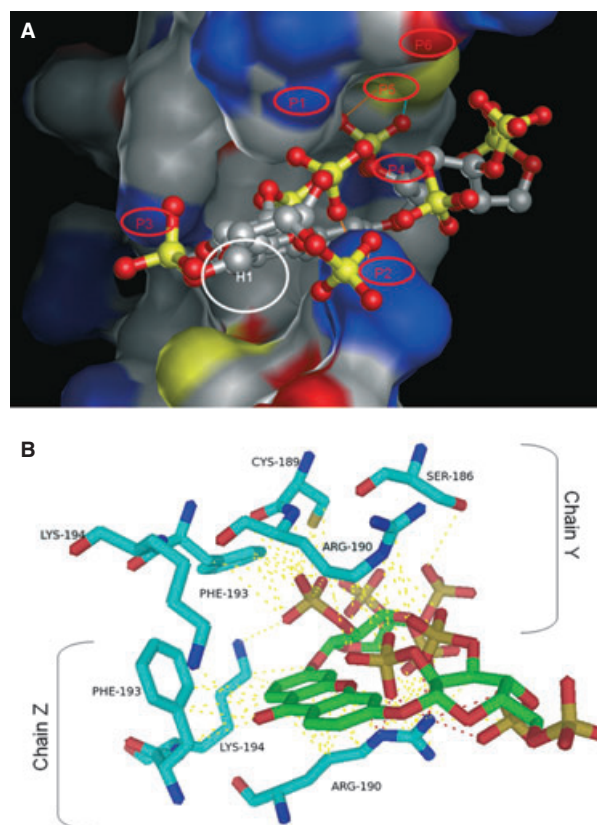


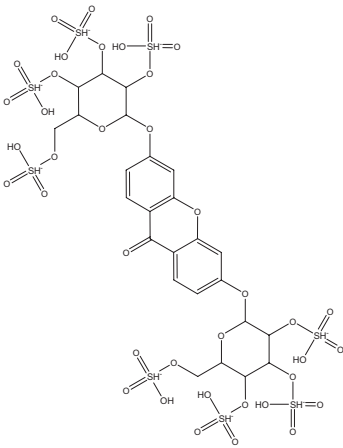
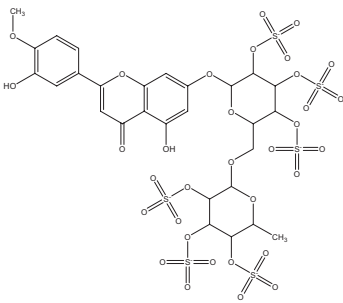
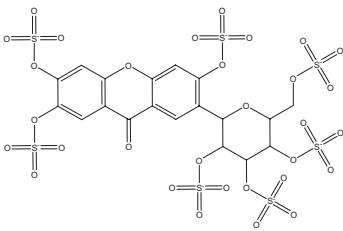
Figure 3: (A) Detail of Zta (pdb: *2c9n*) DNA-binding pocket. Compound **1** is docked in the pocket as an example. Regions P1 to P6 represent polar groups; region H1 represents hydrophobic cavity. Surface is colored by element (red for oxygen, blue for nitrogen, yellow for sulfur, and gray for carbons). (B) Detail of compound **1** bound to Zta (pdb: *2c9n*). Red dashes represent hydrogen interactions, yellow dashes represent other non-covalent interactions.

NH] in ARG190 appears as the principal region for the establishment of H-bond interactions with the ligand. Other polar contacts are established by amino and thiol groups in CYS189 and carbonyl group in SER186. Hydrophobic contacts happen between aromatic ring in PHE193 and hydrocarbon chains in LYS194 and ARG190. Both chains Y and Z contribute to the binding, and several conformations of the ligand inside the binding pocket (with ARG190X and ARG190Y being responsible for H-bonding) are possible and energetically favorable. To understand the binding mode of sulfate within the DNA-binding site of EBNA1 (*1b3t* and *1vhi*), BHRF1 (*1q59*), and Zta (*2c9l* and *2c9n*), compounds **1–3** in complex with the target protein were analyzed and important binding residues are listed in Table 3.

Analysis of the effect of compounds **1–3** in cellular viability

Antiviral drugs should not present cell toxicity. Therefore, the effect of compounds **1–3** on the number of viable

Table 3: Residues involved in the binding of compounds **1–3** on EBNA1 (*1b3t* and *1vhi*), BHRF1(*1q59*), and Zta(*2c9l* and *2c9n*) target proteins

Ligand	Residues involved in the binding				
	<i>1b3t</i>	<i>1vhi</i>	<i>1q59</i>	<i>2c9l</i>	<i>2c9n</i>
 <p style="text-align: center;">1</p>	–	–	–	ARG190y SER189y LYS194z ARG190z	ARG190y
 <p style="text-align: center;">2</p>	–	–	–	ARG190y SER189y ARG183y ARG190z LYS194z SER189z ALA185z	SER186y ASN182y ARG190z SER189z ASN182z
 <p style="text-align: center;">3</p>	ARG469 LYS514 TYR518 ARG521 ARG522 HIS468	–	–	ARG182y ARG187y ARG190y ARG190z	ASN182y ARG190y ARG190z SER186z

EBNA1, Epstein–Barr virus nuclear antigen 1.

cells was evaluated 48 h following the treatment of Raji cells with 20 μM of each tested compound or with the appropriate solvent control (H_2O). Results show that, at the concentration analyzed, all the tested compounds (**1–3**) did not present great cytotoxicity to Raji cells (Figure 4). Indeed, while compound **3** hardly affected the number of viable cells compared with blank treatment (90% of viable cells in relation to blank), compounds **1**

and **2** had only a slight effect on the number of viable cells, reducing viable cell number to 82% or 74%, respectively, which indicates a weak cytotoxic effect to these BL cells. In addition, these compounds had previously been tested in three other tumor cell lines (MCF-7, NCI-H460, and A375-C5), using the sulforhodamine assay, and presented no cytotoxicity (unpublished data, in preparation for publication).

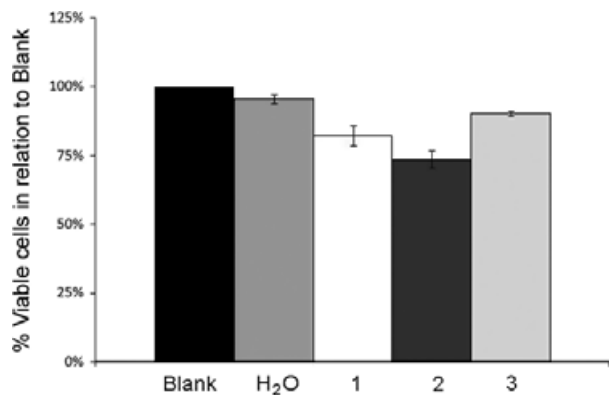


Figure 4: Compounds **1–3** do not greatly affect Raji viable cell number. Raji cells were treated with 20 μM of compounds **1–3**, with their vehicle (H_2O) or with cell culture medium (blank). The number of viable cells was counted with trypan blue, 48 h after treatment with the molecules. Results were analyzed as a percentage of the blank cell number (considering this as 100%) and are the mean \pm SE of three independent experiments.

Analysis of the effect of compounds **1–3** in EBV genome copy number

To verify whether the selected compounds **1–3** had an effect on EBV genome copy number in the Raji cells, viral DNA was analyzed 96 h after the incubation of the cells with 20 μM of each tested compound (or with the solvent, as control). By conventional PCR analysis, EBV DNA was detected, and the resulting bands were quantified by densitometry (by detecting cellular DNA through the amplification of actin DNA and further relating EBV DNA to cellular DNA levels). The results from the densitometry analysis of the EBV DNA load (Figure 5A) were indicative of a reduction in EBV DNA levels in Raji cells following the treatment with compounds **1–3**, when comparing with the control cells (treated with solvent). To confirm these results, experiments were repeated, and EBV DNA load was quantified by real-time PCR (again normalizing for the amount of cellular DNA). Results confirmed the decrease in the EBV DNA load following treatment with compounds **1–3**. Although the levels of decrease were not as high as previously observed by the conventional PCR approach (semi-quantitative), the same trend of decrease was observed (with real-time quantitative PCR) for the three compounds (**1–3**).

Analysis of the effect of compounds **1–3** in LMP1 latent protein expression

Raji cell line has a type III latency EBV infection and may express all the latency viral proteins, such as LMP1. To determine whether the selected compounds (**1–3**) had an effect on the expression of LMP1 in Raji cells, cells were treated for 48 h with 20 μM of each tested compound or with their solvent as control (water). The protein levels of LMP1 (latent viral protein) or actin (as loading control)

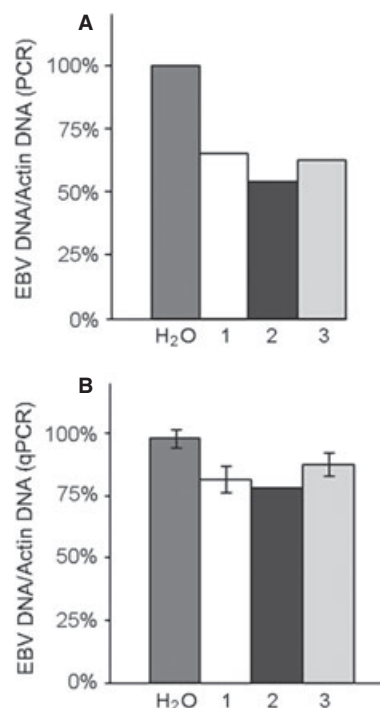


Figure 5: Compounds **1–3** reduced Epstein–Barr virus (EBV) DNA levels in Raji cells. DNA was extracted from Raji cells following 96-h treatment with 20 μM of compounds **1–3** or with their vehicle (H_2O). (A) Densitometry analysis of EBV DNA load following conventional PCR (visualized in agarose gel, data not shown). The intensities of the bands from EBV DNA PCR products were normalized to the intensities of the bands from the respective actin DNA (as internal cellular control). Results, expressed after normalization of the EBV DNA values with the values obtained for cellular actin DNA, were analyzed as percentage of control cells (treated with H_2O) and are the mean of two independent experiments. (B) Real-time quantitative PCR (qPCR) analysis of EBV DNA load. Results, expressed after normalization of the EBV DNA values with the values obtained for cellular actin DNA, were analyzed as percentage of blank cells and represent the mean \pm SE of three independent experiments performed in triplicate (except for compound **2**, which is the mean of only two experiments).

were then analyzed, by Western blot. Results indicate that all the tested compounds (**1–3**) reduced the expression of the latent LMP1 protein, with compound **3** presenting the strongest effect (Figure 6A), which was reproducible in all the independent experiments performed.

To exclude the possibility of these compounds inducing the EBV lytic cycle, as previously observed for some drugs included by some of us (10,13,58), the expression of a lytic protein (EA-D) following treatment with each of the compounds (**1–3**) or with their solvent was analyzed. There were no alterations in the levels of EA-D protein expression (whose increase would indicate lytic reactivation) following the treatment of the Raji cells with each of the tested compounds (**1–3**), thereby confirming that

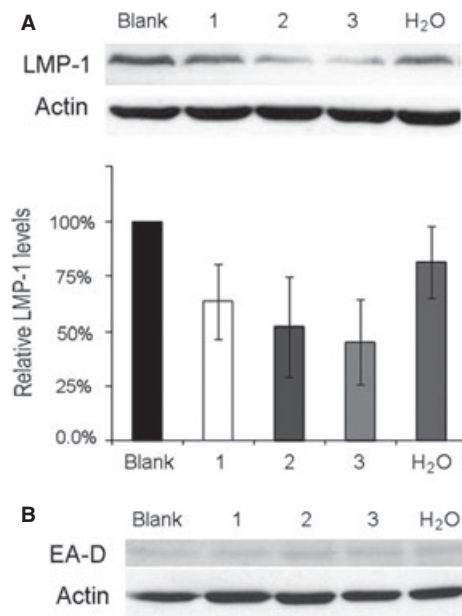


Figure 6: Compounds **1–3** decreased LMP1 viral protein expression in the Raji cell line, but had no effect on viral EA-D expression. Raji cells were treated with 20 μM of compounds **1–3**, with their solvent (H₂O), or with medium only (blank). The expression of latent LMP1 (A) or lytic EA-D (B) proteins was analyzed 48 h after treatment, by Western blot. Actin expression was also analyzed as loading control. Blots are representative of three independent experiments. In (A), the densitometry analysis of the Western blots is shown on the lower panel of the figure. Results are expressed after normalization of the values obtained for the LMP1 with the values obtained for actin and also expressed as percentage of the values obtained for the blank control. Each bar represents the mean \pm SE from three independent experiments.

these compounds did not cause viral reactivation (Figure 6B).

The tested sulfated compounds do not prevent viral reactivation

To determine whether the compounds **1–3** were able not only to interfere with latent EBV but also to prevent EBV lytic reactivation, Raji cells were treated for 48 h with the known lytic inducer TPA and simultaneously treated with 20 μM of each tested compound (or with their solvent). Reactivation of the virus was assessed by analyzing the levels of lytic protein EA-D (and of cellular actin, used as loading control) by Western blot. Results confirmed that TPA induced viral reactivation, as there was an increase in the EA-D protein levels following the treatment of Raji cells with this drug. However, none of the tested compounds, when added to the cells at the same time as TPA, was capable of inhibiting viral reactivation (Figure 7), as the levels of EA-D observed in cells treated with both TPA and with these sulfated compounds were similar to the levels observed following the treatment with TPA alone.

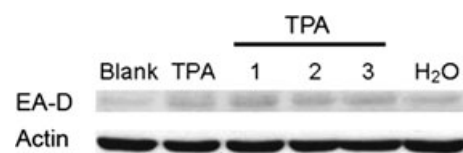


Figure 7: Compounds **1–3** had no effect on viral reactivation induced by 12-*O*-Tetradecanoylphorbol-13-acetate (TPA). Raji cells were treated with the Epstein–Barr virus (EBV) lytic inducer TPA or simultaneously treated with TPA and 20 μM of compounds **1–3**. Control treatments included the vehicle (H₂O) or cell culture medium (blank). The expression of the lytic protein EA-D was analyzed by Western blot. Actin expression was analyzed as loading control. Blot is representative of two independent experiments.

Discussion

In BL, as in the majority of the diseases associated with EBV infection, EBV DNA is maintained as an episome giving rise to a latent infection where no infectious virus are produced. The existing antiviral drugs do not target latent EBV (8), being effective only following induction of lytic EBV reactivation. Thus, some strategies for the treatment of these pathologies are based on the use of lytic EBV inducers, which convert EBV into the lytic form, which is susceptible to the activity of the existing antivirals. However, the resulting increase in the number of viral particles during lytic infection will end in infection of new cells, increasing the likelihood of development of EBV-associated diseases. In fact, the development of EBV-associated lymphomas has already been described in patients with rheumatoid arthritis and polymyositis, following treatment with drugs that induce EBV lytic cycle (11,59).

Therefore, new strategies aiming at latent EBV are being developed, some of them trying to target the EBV episome, while others trying to aim at the EBV viral products or at cellular products that are EBV associated. Major contributions to the design of new therapeutic strategies arise from the association of laboratory studies with computational analysis. In fact, through docking models, it is possible to choose the best molecules that associate with a specific target and to score this association according to their binding affinities (60). By sorting the best molecules (and groups of molecules) that fit a certain model, it is possible to further modify those molecules to optimize and to improve their binding to the selected target. The aim is to reduce large numbers of compounds to smaller subsets that are more likely to contain biologically active compounds (61).

The results obtained by the *in silico* screening indicate that some of the molecules from the CEQUIMED-UP library of compounds may act as possible EBV inhibitors. In fact, using three targets (and for some of them, using different regions from their crystallographic structure as targeted region), from the 97 molecules screened, the sulfated

compounds **1–3** were found to possibly target Zta. One of these small molecules, compound **3**, was also found to possibly target EBNA1. Regarding BHRF1, none of the investigated molecules showed scores that might indicate this protein as their target, therefore showing a need to expand the search for BHRF1 inhibitors to a larger library of molecules. Based on the docking results, we can postulate that Zta protein is probably the preferred target of these sulfated small molecules, and EBNA1 could be a secondary target for compound **3**.

A number of viruses use sites on heparan sulfate (HS) as receptors for binding to cells. Mimics of these sequences are likely to interact with the virus in solution, thereby tying it up and disrupting the viruses interaction with cell surface HS. The HS proteoglycans present in the lymphoid cell surface had already been published as being important in the establishment of interactions with the transcriptional activator EB1/Zta (62,63), which reinforces the selection of these sulfated compounds for further investigation. However, some reports indicate that EBV does not seem to depend on HS for its binding and entry to the host cell. In fact, B-cell lines such as Raji, for which EBV has tropism, are defective for HS expression (64,65). Additionally, sulfated polysaccharides are well known as powerful antiviral drugs (66); nevertheless, sulfated polymeric molecules might only inhibit virus entry and have limited bioavailability. Several studies concerning antiviral activity of sulfated small molecules have been previously described (67–69). For instance, thalassiolins are flavones inhibitors of HIV integrase, in which the sulfate group was found to be a substituent that imparts increased potency against integrase in biochemical assays (68). Another example is lamellarin α -20-sulfate, an HIV-1 integrase inhibitor with a dual mechanism of antiviral action possibly binding to a site composed of multiple integrase domains and found to inhibit HIV entry (69). Nevertheless, the effect of sulfated small molecules in latent EBV infection still needs to be addressed. As sulfated small molecules have proven their antiviral potential by interaction not only with envelope glycoproteins, but also with critical proteins involved in other stages of the viral cycle, compounds **1–3** were selected over other potential hit ligands obtained in the docking studies.

To validate the results obtained in the computational docking analysis, biological studies were performed using the non-producer BL cell line, Raji. This cell line stably maintains the EBV episome copy number (50–60 copies per cell) during long-term culture and presents a type III EBV latency, therefore expressing all the EBV latent proteins (12,70). However, it may reactivate, that is, switch from latency to lytic infection following different stimulus, and lytic proteins may then be produced. Thus, using Raji cells, the study of the antiviral effect of the three selected compounds was carried out by analyzing their effect in EBV DNA load, in the inhibition of latent viral protein expression, and in the inhibition of viral reactivation

induced by TPA. In addition, the fact that these compounds did not present cytotoxicity at the concentrations tested for their antiviral activity is relevant for their possible use as antivirals, as antiviral drugs should be specific and should not affect cell viability. Previous studies have shown the clinical relevance of the monitoring of EBV DNA load for the diagnosis of EBV-associated disorders and for assessment of the efficacy of therapeutic interventions (71). Moreover, following lytic reactivation, a correlation in EBV-infected cells between the levels of lytic proteins and the amount of EBV DNA present has been described (30). By monitoring the EBV viral load following treatment with the three selected small molecules, the objective was to see whether these compounds affected EBV genome copy number, that is, viral DNA load. The fact that all the tested compounds (**1–3**) led to a decrease in the EBV DNA present in Raji cells was a first indication that these molecules were targeting EBV in its latent state or interfering with episome maintenance. Interestingly, antisense-mediated decrease in EBNA1 expression in Raji BL cells was found to concomitantly lead to a reduction in the EBV episome copy number in this cell line (72). Li *et al.* (73), using a strategy similar to ours, virtually screened compounds using the solved crystal structure of EBNA1 with computational docking programs and identified sulfonamides as new inhibitors of EBNA1 transcription. Moreover, some of these compounds also reduced EBV genome copy number in a BL cell line. In addition, through the development of a high-throughput screen for inhibitors of Epstein–Barr virus EBNA1 using homogeneous fluorescence polarization assay, Thompson *et al.* (74) identified three structurally related small molecules that selectively inhibit EBNA1. These three compounds were active in a cell-based assay specific in disrupting EBNA1 transcription repression function, and one was able to reduce EBV genome copy number in Raji cells. Moreover, the use of hydroxyurea (an anticancer drug) to reduce EBV DNA load, although having been successful, has the disadvantage of leading to the accumulation of additional mutations in the cellular genome (18). In this context, the sulfated small molecules revealed herein may serve as a starting point for the development of alternative molecules to hydroxyurea.

Besides affecting EBV DNA load, all the selected compounds **1–3** decreased the levels of LMP1 protein expression (although to different extent). As none of the tested compounds reactivated the virus (did not increase the levels of the lytic EA-D protein), the effects observed resulted from an effect in latent EBV. However, the data obtained so far does not allow drawing conclusions regarding the mechanism of action of these molecules. In fact, although all the investigated (**1–3**) compounds may have Zta as target, no evidence was found that they reduced viral reactivation induced by TPA. This probably indicates that their mechanism of action may be other than the interference with viral reactivation. In fact, although Zta is known to affect the transcription of several genes and its function as



facilitator of viral replication has been thoroughly studied for many years, some new functions for Zta have been published very recently in the literature, namely the ability to stimulate infected resting B cells to proliferate (75).

From the three studied small molecules, compound **3** was the one that presented best results against EBV (observed at the level of decreased expression of LMP1 protein). Interestingly, compound **3** was also the molecule for which the *in silico* screen results showed that it likely targeted both Zta and EBNA1. Thus, it is possible that this compound **3** targets both proteins (EBNA1 and Zta), therefore being more efficient in its antiviral activity.

Although a decrease in the levels of LMP1 has been observed following treatment with all the compounds, these studies do not allow concluding whether this is a specific effect for this type of molecules. In fact, as a reduction in EBV DNA is observed with the three compounds (**1–3**), any alterations observed on the levels of latent proteins may be either a cause or an effect of the decrease in DNA. Therefore, further studies are required to clarify how these molecules interfere with EBV infection. Remarkably, the three top small molecules arising from the *in silico* screening have a sulfate group in their chemical scaffold structure. We could hypothesize an interference of these small molecules (**1–3**) in the virus entry as described for other sulfated compounds (68,69). Sulfated small molecules are expected to preserve some molecular properties of polymeric compounds but with reduced anionic character, higher hydrophobic nature, and feasible synthesis that could ultimately lead to an orally active drug candidate.

The most promising finding of this work was the discovery of xanthonic/flavone sulfated small molecules with some antiviral activity against EBV. By analyzing the possibilities of these molecules, the xanthonic scaffold provides a good starting point to study new EBV inhibitors. As the exact target for these small molecules cannot be pinpointed among the targets assayed computationally, the best strategy would be to consider the possible interaction with EBNA1 (*1b3t* and *1vhj*) or Zta (*2c9l* and *2c9n*). Regarding EBNA1, compound **3** occupies the same place as DNA. Indeed, its polar groups, the ether groups from xanthonic scaffold, and the sulfur groups from lateral chains occupy the same place as purine and pyrimidine moieties placed in the interior of the double-strand DNA helix. We have also noticed that the DNA-binding pocket is only partially occupied. Therefore, the synthesis of molecules that would extend throughout the DNA-binding pocket, like xanthonic derivatives with larger and bulkier chains, or xanthonic dimers with the same substitution pattern, could be an interesting starting point to develop other potential inhibitors of EBV. In what concerns the Zta protein, the studied xanthonic derivatives occupy also the same binding site as DNA. A xanthonic derivative that would extend throughout chains Y and Z, occupying a larger area, should be taken into consideration.

Conclusions

Although further studies are needed to validate these molecules as antiviral compounds against EBV, this study indicates that the *in silico* virtual screening of different compounds may be of added value in the identification of new antiviral molecules. Importantly, as these three possible EBV inhibitors studied are sulfated small molecules, this may be a starting point for further synthetic structural modifications and optimization, as well as for additional computer-assisted methods like 2D and 3D similarity searches. In addition, future studies will be carried out using the molecules presented in this study as well as some of their analogues, to further confirm and increase their potency. Furthermore, we intend to broaden this study to other BL cell lines, including BL virus producer cells, and also to other EBV-associated tumor models, such as NPC. Ultimately, this strategy could result in new antiviral agents against EBV.

Acknowledgments

This work is funded through national funds from FCT – Fundação para a Ciência e a Tecnologia under the project CEQUIMED – PESt-OE/SAU/UI4040/2011, by FEDER funds through the COMPETE program under the project FCOMP-01-0124-FEDER-011057, and by Universidade do Porto and Santander-Totta. IPATIMUP is an Associate Laboratory of the Portuguese Ministry of Science, Technology and Higher Education and is partially supported by FCT. The following grants from FCT were as follows: R. T. Lima (SFRH/BD/21759/2005 and SFRH/BPD/68787/2010), M. Correia-da-Silva (SFRH/BPD/81878/2011), and H. Seca (SFRH/BD/47428/2008). The authors thank K. Choosang and P. Pakkong for unpublished data mentioned in this manuscript.

References

1. Kieff E., Rickinson A.B. (2007) Epstein–Barr virus and its replication. In: Knipe D.M., Howley P.M., editors. Epstein–Barr Virus and Its Replication. Philadelphia: Lippincott-Williams & Wilkins Publishers; p. 2603–2654.
2. Young L.S., Rickinson A.B. (2004) Epstein–Barr virus: 40 years on. *Nat Rev Cancer*;4:757–768.
3. Rawlins D.R., Milman G., Hayward S.D., Hayward G.S. (1985) Sequence-specific DNA binding of the Epstein–Barr virus nuclear antigen (EBNA-1) to clustered sites in the plasmid maintenance region. *Cell*;42:859–868.
4. Reisman D., Sugden B. (1986) Trans activation of an Epstein–Barr viral transcriptional enhancer by the Epstein–Barr viral nuclear antigen 1. *Mol Cell Biol*;6:3838–3846.
5. Lee M.A., Diamond M.E., Yates J.L. (1999) Genetic evidence that EBNA-1 is needed for efficient, stable



- latent infection by Epstein–Barr virus. *J Virol*;73:2974–2982.
6. Ambinder R.F., Shah W.A., Rawlins D.R., Hayward G.S., Hayward S.D. (1990) Definition of the sequence requirements for binding of the EBNA-1 protein to its palindromic target sites in Epstein–Barr virus DNA. *J Virol*;64:2369–2379.
 7. Leight E.R., Sugden B. (2000) EBNA-1: a protein pivotal to latent infection by Epstein–Barr virus. *Rev Med Virol*;10:83–100.
 8. Lin J.-C. (2005) Antiviral therapy for Epstein–Barr virus associated diseases. *Tzu Chi Med J*;17:9.
 9. Feng W.H., Hong G., Delecluse H.J., Kenney S.C. (2004) Lytic induction therapy for Epstein–Barr virus-positive B-cell lymphomas. *J Virol*;78:1893–1902.
 10. Feng W.H., Israel B., Raab-Traub N., Busson P., Kenney S.C. (2002) Chemotherapy induces lytic EBV replication and confers ganciclovir susceptibility to EBV-positive epithelial cell tumors. *Cancer Res*;62:1920–1926.
 11. Feng W.H., Cohen J.I., Fischer S., Li L., Sneller M., Goldbach-Mansky R., Raab-Traub N., Delecluse H.J., Kenney S.C. (2004) Reactivation of latent Epstein–Barr virus by methotrexate: a potential contributor to methotrexate-associated lymphomas. *J Natl Cancer Inst*;96:1691–1702.
 12. Satoh T., Fukuda M., Sairenji T. (2002) Distinct patterns of mitogen-activated protein kinase phosphorylation and Epstein–Barr virus gene expression in Burkitt's lymphoma cell lines versus B lymphoblastoid cell lines. *Virus Genes*;25:15–21.
 13. Lima R.T., Seca H., Bras S., Nascimento M.S., Vasconcelos M.H. (2011) Treatment of Akata EBV-positive cells with doxorubicin causes more EBV reactivation than treatment with etoposide. *Chemotherapy*;57:195–203.
 14. De Clercq E. (2004) Antivirals and antiviral strategies. *Nat Rev Microbiol*;2:704–720.
 15. Kenney S. (2006) Theodore E. Woodward Award: development of novel, EBV-targeted therapies for EBV-positive tumors. *Trans Am Clin Climatol Assoc*;117: 55–73; discussion 73–54.
 16. Chodosh J., Holder V.P., Gan Y.J., Belgaumi A., Sample J., Sixbey J.W. (1998) Eradication of latent Epstein–Barr virus by hydroxyurea alters the growth-transformed cell phenotype. *J Infect Dis*;177:1194–1201.
 17. Slobod K.S., Taylor G.H., Sandlund J.T., Furth P., Helton K.J., Sixbey J.W. (2000) Epstein–Barr virus-targeted therapy for AIDS-related primary lymphoma of the central nervous system. *Lancet*;356:1493–1494.
 18. Hanft V.N., Fruchtman S.R., Pickens C.V., Rosse W.F., Howard T.A., Ware R.E. (2000) Acquired DNA mutations associated with in vivo hydroxyurea exposure. *Blood*;95:3589–3593.
 19. Kenney J.L., Guinness M.E., Reiss M., Lacy J. (2001) Antisense to the Epstein–Barr virus (EBV)-encoded latent membrane protein 1 (LMP-1) sensitizes EBV-immortalized B cells to transforming growth factor-beta and chemotherapeutic agents. *Int J Cancer*;91:89–98.
 20. Masciarelli S., Mattioli B., Galletti R., Samoggia P., Chichiarelli S., Mearini G., Mattia E. (2002) Antisense to Epstein Barr Virus-encoded LMP1 does not affect the transcription of viral and cellular proliferation-related genes, but induces phenotypic effects on EBV-transformed B lymphocytes. *Oncogene*;21:4166–4170.
 21. Rechsteiner M.P., Berger C., Weber M., Sigrist J.A., Nadal D., Bernasconi M. (2007) Silencing of latent membrane protein 2B reduces susceptibility to activation of lytic Epstein–Barr virus in Burkitt's lymphoma Akata cells. *J Gen Virol*;88:1454–1459.
 22. Iwase Y., Takemura Y., Ju-ichi M., Ito C., Furukawa H., Kawai S., Yano M., Mou X.Y., Takayasu J., Tokuda H., Nishino H. (2000) Inhibitory effect of flavonoids from citrus plants on Epstein–Barr virus activation and two-stage carcinogenesis of skin tumors. *Cancer Lett*;154:101–105.
 23. Iwase Y., Takemura Y., Ju-ichi M., Mukainaka T., Ichishi E., Ito C., Furukawa H., Yano M., Tokuda H., Nishino H. (2001) Inhibitory effect of flavonoid derivatives on Epstein–Barr virus activation and two-stage carcinogenesis of skin tumors. *Cancer Lett*;173:105–109.
 24. Ito C., Itoigawa M., Tan H.T., Tokuda H., Yang Mou X., Mukainaka T., Ishikawa T., Nishino H., Furukawa H. (2000) Anti-tumor-promoting effects of isoflavonoids on Epstein–Barr virus activation and two-stage mouse skin carcinogenesis. *Cancer Lett*;152:187–192.
 25. Chang L.K., Wei T.T., Chiu Y.F., Tung C.P., Chuang J.Y., Hung S.K., Li C., Liu S.T. (2003) Inhibition of Epstein–Barr virus lytic cycle by (-)-epigallocatechin gallate. *Biochem Biophys Res Commun*;301:1062–1068.
 26. Ito C., Itoigawa M., Furukawa H., Rao K.S., Enjo F., Bu P., Takayasu J., Tokuda H., Nishino H. (1998) Xanthenes as inhibitors of Epstein–Barr virus activation. *Cancer Lett*;132:113–117.
 27. Chang F.R., Hsieh Y.C., Chang Y.F., Lee K.H., Wu Y.C., Chang L.K. (2010) Inhibition of the Epstein–Barr virus lytic cycle by moronic acid. *Antiviral Res*;85:490–495.
 28. Nakagawa-Goto K., Yamada K., Taniguchi M., Tokuda H., Lee K.H. (2009) Cancer preventive agents 9. Betulinic acid derivatives as potent cancer chemopreventive agents. *Bioorg Med Chem Lett*;19:3378–3381.
 29. Lin J.C., Cherng J.M., Hung M.S., Baltina L.A., Baltina L., Kondratenko R. (2008) Inhibitory effects of some derivatives of glycyrrhizic acid against Epstein–Barr virus infection: structure-activity relationships. *Antiviral Res*;79:6–11.
 30. Lin J.C. (2003) Mechanism of action of glycyrrhizic acid in inhibition of Epstein–Barr virus replication in vitro. *Antiviral Res*;59:41–47.
 31. Kellenberger E., Muller P., Schalon C., Bret G., Foata N., Rognan D. (2006) sc-PDB: an annotated database



- of druggable binding sites from the Protein Data Bank. *J Chem Inf Model*;46:717–727.
32. Zsoldos Z., Reid D., Simon A., Sadjad B.S., Johnson A.P. (2006) eHiTS: an innovative approach to the docking and scoring function problems. *Curr Protein Pept Sci*;7:421–435.
 33. Zsoldos Z., Reid D., Simon A., Sadjad S.B., Johnson A.P. (2007) eHiTS: a new fast, exhaustive flexible ligand docking system. *J Mol Graph Model*;26:198–212.
 34. Froimowitz M. (1993) HyperChem: a software package for computational chemistry and molecular modeling. *Biotechniques*;14:1010–1013.
 35. Vigers G.P., Rizzi J.P. (2004) Multiple active site corrections for docking and virtual screening. *J Med Chem*;47:80–89.
 36. O'Boyle N.M., Morley C., Hutchison G.R. (2008) Pybel: a Python wrapper for the OpenBabel cheminformatics toolkit. *Chem Cent J*;2:5.
 37. Ordog R. (2008) PyDeT, a PyMOL plug-in for visualizing geometric concepts around proteins. *Bioinformatics*;23:346–347.
 38. Pettersen E.F., Goddard T.D., Huang C.C., Couch G.S., Greenblatt D.M., Meng E.C., Ferrin T.E. (2004) UCSF Chimera—a visualization system for exploratory research and analysis. *J Comput Chem*;25:1605–1612.
 39. Voigt J.H., Bienfait B., Wang S., Nicklaus M.C. (2001) Comparison of the NCI open database with seven large chemical structural databases. *J Chem Inf Comput Sci*;41:702–712.
 40. Costa E., Sousa E., Nazareth N., Nascimento M.S.J., Pinto M.M.M. (2010) Synthesis of xanthenes and benzophenones as inhibitors of tumor cell growth. *Lett Drug Des Discovery*;7:487–493.
 41. Correia-da-Silva M., Sousa E., Duarte B., Marques F., Carvalho F., Cunha-Ribeiro L.M., Pinto M.M.M. (2011) Flavonoids with an oligopolysulfated moiety: a new class of anticoagulant agents. *J Med Chem*;54:95–106.
 42. Correia-da-Silva M., Sousa E., Duarte B., Marques F., Carvalho F., Cunha-Ribeiro L.M., Pinto M.M.M. (2011) Polysulfated xanthenes: multipathway development of a new generation of dual anticoagulant/antiplatelet agents. *J Med Chem*;54:5373–5384.
 43. Son Y.O., Choi K.C., Lee J.C., Kook S.H., Lee S.K., Takada K., Jang Y.S. (2006) Involvement of caspase activation and mitochondrial stress in taxol-induced apoptosis of Epstein–Barr virus-infected Akata cells. *Biochim Biophys Acta*;1760:1894–1902.
 44. Tafuku S., Matsuda T., Kawakami H., Tomita M., Yagita H., Mori N. (2006) Potential mechanism of resistance to TRAIL-induced apoptosis in Burkitt's lymphoma. *Eur J Haematol*;76:64–74.
 45. Lu F., Weidmer A., Liu C.G., Volinia S., Croce C.M., Lieberman P.M. (2008) Epstein–Barr virus-induced miR-155 attenuates NF-kappaB signaling and stabilizes latent virus persistence. *J Virol*;82:10436–10443.
 46. Lima R.T., Seca H., Soares P., Nascimento M.S., Vasconcelos M.H. (2011) EBV interferes with the sensitivity of Burkitt lymphoma Akata cells to etoposide. *J Cell Biochem*;112:200–210.
 47. Palmeira A., Paiva A., Sousa E., Seca H., Almeida G.M., Lima R.T., Fernandes M.X., Pinto M., Vasconcelos M.H. (2010) Insights into the in vitro antitumor mechanism of action of a new pyranoxanthone. *Chem Biol Drug Des*;76:43–58.
 48. Diabata M., Enzinger E.M., Monroe J.E., Kilkuskie R.E., Field A.K., Mulder C. (1996) Antisense oligodeoxynucleotides against the BZLF1 transcript inhibit induction of productive Epstein–Barr virus replication. *Antiviral Res*;29:243–260.
 49. Prang N., Wolf H., Schwarzmann F. (1999) Latency of Epstein–Barr virus is stabilized by antisense-mediated control of the viral immediate-early gene BZLF-1. *J Med Virol*;59:512–519.
 50. Chang Y., Chang S.S., Lee H.H., Doong S.L., Takada K., Tsai C.H. (2004) Inhibition of the Epstein–Barr virus lytic cycle by Zta-targeted RNA interference. *J Gen Virol*;85:1371–1379.
 51. Oudejans J.J., van den Brule A.J., Jiwa N.M., de Bruin P.C., Ossenkoppele G.J., van der Valk P., Walboomers J.M., Meijer C.J. (1995) BHRF1, the Epstein–Barr virus (EBV) homologue of the BCL-2 protooncogene, is transcribed in EBV-associated B-cell lymphomas and in reactive lymphocytes. *Blood*;86:1893–1902.
 52. Herman M.D., Nyman T., Welin M., Lehtio L., Flodin S., Tresaugues L., Kotenyova T., Flores A., Nordlund P. (2008) Completing the family portrait of the anti-apoptotic Bcl-2 proteins: crystal structure of human Bfl-1 in complex with Bim. *FEBS Lett*;582:3590–3594.
 53. Kvensakul M., Wei A.H., Fletcher J.I., Willis S.N., Chen L., Roberts A.W., Huang D.C., Colman P.M., (2010) Structural basis for apoptosis inhibition by Epstein–Barr virus BHRF1. *PLoS Pathog*;6:e1001236.
 54. Huang Q., Petros A.M., Virgin H.W., Fesik S.W., Olejniczak E.T. (2003) Solution structure of the BHRF1 protein from Epstein–Barr virus, a homolog of human Bcl-2. *J Mol Biol*;332:1123–1130.
 55. Bochkarev A., Barwell J.A., Pfuertner R.A., Furey W. Jr, Edwards A.M., Frappier L. (1995) Crystal structure of the DNA-binding domain of the Epstein–Barr virus origin-binding protein EBNA 1. *Cell*;83:39–46.
 56. Valnet-Rabier M.B., Challier B., Thiebault S., Angonin R., Marguerite G., Mouglin C., Kantelip B., Deconinck E., Cahn J.Y., Fest T. (2005) c-Flip protein expression in Burkitt's lymphomas is associated with a poor clinical outcome. *Br J Haematol*;128:767–773.
 57. Petosa C., Morand P., Baudin F., Moulin M., Artero J.B., Muller C.W. (2006) Structural basis of lytic cycle activation by the Epstein–Barr virus ZEBRA protein. *Mol Cell*;21:565–572.
 58. Hsu C.H., Hergenahn M., Chuang S.E., Yeh P.Y., Wu T.C., Gao M., Cheng A.L. (2002) Induction of Epstein–Barr virus (EBV) reactivation in Raji cells by



- doxorubicin and cisplatin. *Anticancer Res*;22:4065–4071.
59. Rao S.P., Rechsteiner M.P., Berger C., Sigrist J.A., Nadal D., Bernasconi M. (2007) Zebularine reactivates silenced E-cadherin but unlike 5-Azacytidine does not induce switching from latent to lytic Epstein–Barr virus infection in Burkitt's lymphoma Akata cells. *Mol Cancer*;6:3.
 60. Palmeira A., Rodrigues F., Sousa E., Pinto M., Vasconcelos M.H., Fernandes M.X. (2011) New uses for old drugs: pharmacophore-based screening for the discovery of P-glycoprotein inhibitors. *Chem Biol Drug Des*;78:57–72.
 61. Guido R.V., Oliva G., Andricopulo A.D. (2008) Virtual screening and its integration with modern drug design technologies. *Curr Med Chem*;15:37–46.
 62. Mahot S., Fender P., Vives R.R., Caron C., Perrissin M., Gruffat H., Sergeant A., Drouet E. (2005) Cellular uptake of the EBV transcription factor EB1/Zta. *Virus Res*;110:187–193.
 63. Berry D., Lynn D.M., Berry E., Sasisekharan R., Langer R. (2006) Heparin localization and fine structure regulate Burkitt's lymphoma growth. *Biochem Biophys Res Commun*;348:850–856.
 64. Jarousse N., Chandran B., Coscoy L. (2008) Lack of heparan sulfate expression in B-cell lines: implications for Kaposi's sarcoma-associated herpesvirus and murine gammaherpesvirus 68 infections. *J Virol*;82:12591–12597.
 65. Nasimuzzaman M., Persons D.A. (2012) Cell membrane-associated heparan sulfate is a receptor for prototype foamy virus in human, monkey, and rodent cells. *Mol Ther*;20:1158–1166.
 66. Cos P., Maes L., Vanden Berghe D., Hermans N., Pieters L., Vlietinck A. (2004) Plant substances as anti-HIV agents selected according to their putative mechanism of action. *J Nat Prod*;67:284–293.
 67. Sousa E., da Silva M.C., Pinto M.M.M. (2009) Sulfated flavonoids: nature playing with the hydrophilic-hydrophobic balance. In: Brahmachari G., editor. *Sulfated Flavonoids: Nature Playing with the Hydrophilic-Hydrophobic Balance*. New Delhi, India: Narosa Publishing House PVT. LTD; p. 392–462.
 68. Rowley D.C., Hansen M.S.T., Rhodes D., Sotriffer C.A., Ni H., McCammon A., Bushman F.D., Fenical W. (2002) Thalassiolins A-C: new marine-derived inhibitors of HIV cDNA integrase. *Bioorg Med Chem*;10:3619–3625.
 69. Reddy M.V.R., Rao M.R., Rhodes D., Hansen M.S.T., Rubins K., Bushman F.D., Venkateswarlu Y., Faulkner D.J. (1999) Lamellarin α 20-Sulfate, an inhibitor of HIV-1 integrase active against HIV-1 virus in cell culture. *J Med Chem*;42:1901–1907.
 70. Jiang R., Zhang J.L., Satoh Y., Sairenji T. (2004) Mechanism for induction of hydroxyurea resistance and loss of latent EBV genome in hydroxyurea-treated Burkitt's lymphoma cell line Raji. *J Med Virol*;73:589–595.
 71. Stevens S.J., Pronk I., Middeldorp J.M. (2001) Toward standardization of Epstein–Barr virus DNA load monitoring: unfractionated whole blood as preferred clinical specimen. *J Clin Microbiol*;39:1211–1216.
 72. Pagano J.S., Jimenez G., Sung N.S., Raab-Traub N., Lin J.C. (1992) Epstein–Barr viral latency and cell immortalization as targets for antisense oligomers. *Ann N Y Acad Sci*;660:107–116.
 73. Li N., Thompson S., Schultz D.C., Zhu W., Jiang H., Luo C., Lieberman P.M. (2010) Discovery of selective inhibitors against EBNA1 via high throughput in silico virtual screening. *PLoS One*;5:e10126.
 74. Thompson S., Messick T., Schultz D.C., Reichman M., Lieberman P.M. (2010) Development of a high-throughput screen for inhibitors of Epstein–Barr virus EBNA1. *J Biomol Screen*;15:1107–1115.
 75. Kalla M., Schmeinck A., Bergbauer M., Pich D., Hammerschmidt W. (2010) AP-1 homolog BZLF1 of Epstein–Barr virus has two essential functions dependent on the epigenetic state of the viral genome. *Proc Natl Acad Sci USA*;107:850–855.

Supporting Information

Additional Supporting Information may be found in the online version of this article:

Table S1. Docking scores of random NCI compounds on EBNA1 (*1b3t* and *1vhj*), BHRF1(*1q59*), and Zta (*2c9l* and *2c9n*) target proteins.